

the estimate derived from π^+ and π^- range data.²

Note added in proof. A tabular presentation of the functions I , F , and L is given in a paper to be submitted to Atomic Data by the authors, as yet unpublished.

*Research sponsored by the U. S. Atomic Energy Commission under contract with Union Carbide Corp.

¹W. H. Barkas, J. W. Dyer, and H. H. Heckman, Phys. Rev. Letters **11**, 26 (1963); **11**, 138(E) (1963).

²H. H. Heckman and P. J. Lindstrom, Phys. Rev. Letters **22**, 871 (1969), and references cited therein.

³H. H. Andersen, H. Simonsen, and H. Sørensen, Nucl. Phys. **A125**, 171 (1969).

⁴N. Bohr, Kgl. Danske Videnskab. Selskab, Mat.-Fys. Medd. **18**, No. 8 (1948).

⁵If the impact parameter separating these two types of collisions is chosen by the criterion that the energy to a free electron at this impact parameter is equal to the binding energy of the struck electron, one obtains a stopping-power formula which is in disagreement with Bethe's quantum-mechanical formula. The disagreement arises from the fact that usually such a choice of intermediate impact parameter violates the uncertainty principle. Proper consideration of the uncertainty principle in our problem requires that we limit the range of a_ω to values larger than \hbar/mv_1 .

⁶See, e.g., P. Gombas, *Die statistische Theorie des*

ACKNOWLEDGMENT

We want to thank V. E. Anderson for his work on the computer evaluation of the various functions required in this theory.

Atoms und ihre Anwendungen (Springer-Verlag, Berlin, 1949), p. 74.

⁷J. Lindhard and M. Scharff, Kgl. Danske Videnskab. Selskab, Mat.-Fys. Medd. **27**, No. 15 (1953).

⁸W. Brandt and S. Lundqvist, Phys. Rev. **139**, A612 (1965).

⁹J. Lindhard and M. Scharff, in *Penetration of Charged Particles in Matter*, edited by E. A. Uehling, National Academy of Sciences-National Research Council Publication No. 752 (U. S. GPO, Washington, D. C., 1960), p. 49.

¹⁰W. Brandt, J. Lindhard, and M. Scharff, in *Proceedings of the Second International Conference on the Physics of Electronic and Atomic Collisions, Boulder, 1961* (Benjamin, New York, 1961), p. 11.

¹¹W. Brandt, L. Eder, and S. Lundqvist, J. Quant. Spectry. Radiative Transfer **7**, 185 (1967).

¹²R. M. Sternheimer, Phys. Rev. **145**, 247 (1966).

¹³See, e.g., E. Bonderup, Kgl. Danske Videnskab. Selskab, Mat.-Fys. Medd. **35**, No. 17 (1967) for a more detailed treatment of shell corrections using statistical models of the atoms.

Temperature-Independent Spin-Lattice Relaxation Time in Metals at Very Low Temperatures*

F. Bacon, J. A. Barclay,† W. D. Brewer,‡ D. A. Shirley, and J. E. Templeton§

*Department of Chemistry and Lawrence Radiation Laboratory,
University of California, Berkeley, California 94720*

(Received 10 June 1971)

The formalism of nuclear spin-lattice relaxation at low temperatures is developed, leading to a new relaxation time T_μ and a straightforward method of interpreting very-low-temperature relaxation data. Data for ^{60}Co in Fe, Ni, and Co hosts and for ^{56}Co in Fe are summarized. The use of NMR in oriented nuclei for determining relaxation times is discussed, and some comments are made on the role of frequency modulation in NMR experiments with oriented nuclei.

I. INTRODUCTION

Nuclear magnetic resonance in oriented nuclei (NMR/ON), in which resonance is detected through the distribution of nuclear radiations, was suggested by Bloembergen and Temmer¹ and first observed in nuclei oriented by thermal-equilibrium methods by Matthias and Holliday.² It was used to study relaxation in ferromagnetic metals,³ a phenomenon that has also been studied by nonresonant methods.⁴

In 1964 Cameron *et al.*⁵ suggested that, for nuclei

relaxing in a metal through interaction with conduction electrons, the spin-lattice relaxation time T_1 will approach a constant value at temperatures low enough that the magnetic quantum γH is larger than kT . This effect was observed by Brewer *et al.*, who reported it in abbreviated form in 1968.⁶ These authors made a detailed interpretation of their relaxation data in terms of simple rate equations, finding multiexponential decay of the orientation parameters.^{7,8} They found that T_1 was no longer a useful relaxation time at very low temperatures, however, and their data in $^{60}\text{CoFe}$

were interpreted in terms of a single-exponential decay constant.

The body of this paper is divided into three parts. Section II contains a detailed discussion of the rate-equation approach to a relaxation theory for oriented nuclei, with emphasis on the physical significance of the single-exponential fit at very low temperatures. Several applications to experimental data are given in Sec. III. Section IV contains a brief discussion of the extent to which resonant destruction of nuclear orientation may be achieved through frequency modulation.

II. RELAXATION THEORY

The theory of longitudinal, or spin-lattice, relaxation of oriented nuclei is discussed in this section. The effect of relaxation on the time evolution of statistical tensors in the high-temperature limit is reviewed and its modifications for finite temperatures is considered. For nuclei in metals relaxing through $A\vec{S}\cdot\vec{I}$ interactions with conduction electrons, it is shown that the characteristic *single-exponential* relaxation time in the low-temperature limit (later denoted by T_μ , not to be confused with T_1) is temperature independent and equal to $kC/h\nu I$, where C is the high-temperature Korringa constant ($C = T_1 T$) and ν is the Larmor frequency.

The rate-equation interpretation is described below essentially as it was originally used by Brewer *et al.*⁶⁻⁸ Two other derivations are now available. Using the Liouville-space formalism, Gabriel⁹ developed a general theory of relaxation which gives the results discussed below as a special case. More recently Hartmann-Boutron and Spanjaard^{10,11} have also discussed this problem, obtaining the same results. Two other analyses of experimental measurements—in $^{60}\text{CoCo}$ ¹² and in $^{60}\text{CoFe}$ and $^{60}\text{CoNi}$ ¹³—have also been made. These later theoretical approaches⁹⁻¹¹ are more general than ours. They can easily treat cases entailing transverse relaxation, for example. In application to the present problem, however, only longitudinal relaxation is involved, and the three approaches give identical equations. Thus we shall retain the simpler formulation of Brewer *et al.*⁶⁻⁸

A. The Question of Spin Temperature in Ferromagnetic Metals

Spin systems relax differently when a spin temperature exists than when one does not. Although both cases are treated below, it seems useful to discuss first whether spin temperatures are expected in NMR/ON experiments.

Moriya's theoretical work¹⁴ on relaxation in ferromagnetic metals showed that the relation $T_1 = T_2$ should hold, thereby precluding the existence of a spin temperature T_S , but early measurements on

stable isotopes indicated $T_2 < T_1$. Therefore the first relaxation work with oriented nuclei was interpreted under the assumption that a T_S existed.³ In 1967 Walstedt¹⁵ reported spin-echo measurements on several stable nuclei which showed definitively that $T_2 \approx T_1$, and subsequent analyses⁶⁻⁸ have all been made with no spin-temperature assumption. It has been pointed out that the observation of relaxation in oriented nuclei could provide a definitive test of the existence of a spin temperature in these systems.¹⁶ This follows because the simultaneous measurement of the time dependence of several statistical tensors would provide data that were extremely sensitive to deviations of substate populations from a spin-temperature distribution. Unfortunately it is experimentally difficult to set up initial conditions that are both reliably known and appropriate for testing the T_S hypothesis. The experiments to date have been done under conditions that were not conducive to such tests,^{6,7,13} and the results could be fitted either with or without assuming that a spin temperature exists. While it is very unlikely that the systems studied to date by nuclear orientation can have spin temperatures, this question has not really been tested experimentally. It is also probable that spin systems that *do* have spin temperatures will be studied by nuclear orientation in the future. For these two reasons an expression for the time evolution of the spin temperature is given below.

B. Transition Probabilities: Analogy with Two-Level Radiative Systems

Let us assume that spin-lattice relaxation occurs via an interaction with the conduction electrons, of the form

$$A\vec{I}\cdot\vec{S} = AS_z I_z + \frac{1}{2}A(S_+ I_- + S_- I_+) , \quad (1)$$

and that first-order perturbation theory is applicable. Here \hat{S} is an effective electron-spin operator that can be related to either the orbital or spin operator of conduction electrons, or to both. The discussion below is quite general, requiring only that the nuclei relax by exchanging energy with a degenerate Fermi gas, via magnetic-dipole transitions. If the nuclear energy levels are equally spaced by $h\nu$ and the $|m = -I\rangle$ states lies lowest, we may write for the transition probabilities between states $|m\rangle$ and $|m+1\rangle$

$$W_{m,m+1} = Bh\nu[I(I+1) - m(m+1)]/(e^{x_L} - 1) , \quad (2)$$

$$W_{m+1,m} = Bh\nu[I(I+1) - m(m+1)]/(1 - e^{-x_L}) .$$

Here B is a constant that contains various numerical factors including the density of states at the Fermi energy, and $x_L = h\nu/kT_L$. It is easily shown, by choosing $I = \frac{1}{2}$, substituting into Eq. (2), and comparing with the rate equations in the high-tem-

perature limit, that $B = (2kC)^{-1}$, where C is the high-temperature Korringa constant. Relation (2) was given in slightly different form by Brewer *et al.*⁶ and follows from the expressions given by Cameron *et al.*⁵

The appearance of the Bose-Einstein distribution function $1/(e^{xL} - 1)$ in $W_{m,m\pm 1}$ suggests that the above transition probabilities should possess an interesting analogy with the radiation problem. Of course this is also expected because the states $|m\rangle$ and $|m+1\rangle$ could be connected by the emission and absorption of photons. In the case of magnetic relaxation they are in fact connected by spin-flip excitations in the conduction electrons, i. e., by spin changes $\Delta S = \pm 1$. These excitations clearly have boson character. In the case of nuclear-quadrupole relaxation the boson character is even more obvious, since in this case relaxation processes are accompanied by emission or absorption of lattice phonons which clearly obey Bose statistics. At absolute zero there are no more lattice phonons to absorb but a nucleus can still relax by exciting a phonon; i. e., spontaneous emission remains.

We can rewrite $W_{m,m\pm 1}$ as follows:

$$W_{m+1,m} = \frac{h\nu}{2kC} [I(I+1) - m(m+1)] \left(\frac{1}{(e^{xL} - 1)} + 1 \right) \\ = W_{m,m+1} + \frac{h\nu}{2kC} [I(I+1) - m(m+1)]. \quad (3)$$

Thus the downward transition probability contains two parts, a temperature-dependent part which is equal to the upward probability (in analogy to stimulated emission and absorption) and a temperature-independent part, analogous to spontaneous emission. Here temperature plays a role analogous to the occupation of the radiation field in photon processes. The appearance of stimulated and spontaneous transition probabilities is in fact a general property of transitions whose quanta of excitation obey Bose statistics and are thus more likely to enter states which are already occupied.

C. Relaxation with Spin Temperature

At high temperatures ($kT \gg$ nuclear substate level spacings) the familiar expression³

$$\dot{\beta} = -(1/T_1)(\beta - \beta_L)$$

is approximately correct. Here $\beta = 1/kT_S$ and $\beta_L = 1/kT_L$, where T_S and T_L are the spin and lattice temperatures, respectively. At lower temperatures this relation breaks down, and it is necessary to go back to the master equation,¹⁷

$$\dot{\rho}_m = \sum_n (\rho_n W_{nm} - \rho_m W_{mn}). \quad (4)$$

Here ρ_m is a diagonal element of the density matrix and W_{mn} is the transition probability from state $|m\rangle$ to state $|n\rangle$. Starting from Eq. (4), at least

three papers^{13,16,18} have quoted expressions for $\dot{\beta}$. Shirley¹⁶ gave an equation that is not valid at very low temperatures. Spanjaard *et al.*¹³ give an expression that should be valid at all temperatures, but their $\dot{\beta}$ is given implicitly in several equations. Jauho and Pirilä¹⁸ give expressions for the nuclear polarization and alignment which contain $\dot{\beta}$ implicitly. A derivation following the procedure given by Slichter¹⁷ but valid for all temperatures leads to the following result:

$$h\nu \dot{\beta} = \dot{x} = \frac{h\nu}{2kC} \frac{e^{-xL} - e^{-x}}{1 - e^{-xL}} \frac{I(I+1) - \langle m^2 \rangle - \langle m \rangle}{\langle m \rangle^2 - \langle m \rangle} \quad (5)$$

or, expressing the sums on m as Brillouin functions,

$$\dot{x} = \frac{h\nu}{2kC} \frac{e^{-xL} - e^{-x}}{1 - e^{-xL}} \frac{I+1 - B'_I(x) - IB_I^2(x) + B_I(x)}{B'_I(x)}, \quad (6)$$

where

$$B_I(x) = \frac{2I+1}{2I} \coth\left(\frac{(2I+1)}{2}x\right) - \frac{1}{2I} \coth\frac{x}{2}$$

and

$$B'_I(x) = \frac{d[B_I(x)]}{dx}.$$

In a system for which $h\nu$, I , and C are known, and for which a given lattice temperature exists, Eq. (5) is a useful differential equation relating the spin temperature to its time derivative. It may be solved numerically. In the high- and low-temperature limits, for $x - x_L \ll 1$, Eq. (5) goes to

$$\lim \dot{\beta} = (1/T_1)(\beta_L - \beta) \quad \text{as } T_L \rightarrow \infty, \quad (7)$$

$$\lim \dot{\beta} = (1/T_\mu)(\beta_L - \beta) \quad \text{as } T_L \rightarrow 0, \quad (8)$$

where $T_\mu = kC/h\nu I$, a temperature-independent relaxation constant that is discussed in Sec. IIG.

D. Relaxation with No Spin Temperature

For most experiments in which nuclear radiations are used to study nuclear spin-lattice relaxation, the active nuclei are present in such low concentration that they may be taken as independent. Let us again consider nuclei in a metal, subject to a relaxation interaction of the form $\frac{1}{2}A(S_+I_- + S_-I_+)$ arising from conduction electrons. The time evolution of the set of $(2I+1)$ diagonal elements of the density matrix $\{\rho_m\}$ is still given by Eqs. (2)–(4), but without a spin-temperature constraint. Rather than dealing with the $\{\rho_m\}$ themselves, it is convenient to define a new set of quantities $\{p_m\}$ that measure the deviation of the elements ρ_m from their equilibrium values ρ_m^0 ,

$$p_m = \rho_m - \rho_m^0. \quad (9)$$

Since $\dot{\rho}_m = 0$ at equilibrium, Eqs. (4) and (9) may be combined to give

roots are simply the diagonal elements of F_{LT} . Thus the low-temperature limiting decay constants are, for integral I : 0 (appearing once), $I(h\nu/kC)$, $(2I-1)(h\nu/kC)$, $\dots \frac{1}{2}I(I+1)(h\nu/kC)$ (each appearing twice). The two smallest nonzero rate constants, having the values $h\nu/kC$, will strongly influence the rate of change of *all* observables as the lattice temperature approaches absolute zero, provided that secular equilibrium is established. In most practical experimental situations the initial conditions will lead to secular equilibrium rather quickly, and T'_1 as obtained from a single-exponential analysis will approach its low-temperature limiting value

$$\lim T'_1 = kC/h\nu I \quad \text{as } T \rightarrow 0 \quad (42)$$

reasonably closely at a relatively high temperature. Of course the actual rate characterized by $1/T'_1$ tends to be slower than $1/T_\mu$, because the other transition rates are not very much faster than $1/T_\mu$. It is important to know, in a given experiment, whether or not secular equilibrium has been established. This may be done by plotting $\ln W(\theta, t)$ against t for each run, and checking for constancy in the slope. A final test is provided by inspecting the values of T'_1 , as obtained from least-squares analysis, to see whether they do in fact approach constancy as T decreases. We emphasize these precautions because for certain sets of initial conditions careless data analysis can lead to erroneous results. For example, in some cases T'_1 obtained from a single-exponential fit can exhibit a maximum before approaching its limiting value. Alternatively a multiexponential analysis may be made to obtain the smallest nonzero eigenvalue of F . However the analysis is done, the final result is the fundamental spin-lattice relaxation time

$$T_\mu = \frac{kC}{h\nu I} = \frac{kC}{\mu H} = \lim_{T \rightarrow 0} T'_1 \quad (43)$$

We shall call T_μ the *magnetic spin-lattice relaxation time*. In the low-temperature limit T_μ plays a role which is similar to, but more general than, that of T_1 in the high-temperature limit. The following properties of T_μ are of interest:

(i) In the low-temperature limit, and provided that the spins are close enough to equilibrium that all ρ_m can be neglected for $m \geq 2 - I$, T_μ becomes a true relaxation time for all observables. Since $\dot{\rho}_{-I+1} = -(1/T_\mu)\rho_{-I+1}$ in this limit, it follows that

$$\lim[\rho_0^\lambda(t) - \rho_0^\lambda(eq)] = -(1/T_\mu)[\rho_0^\lambda(t) - \rho_0^\lambda(eq)]$$

for all tensor ranks λ under these conditions. This follows because the tensors ρ_0^λ are linear in the ρ_m [Eq. (19)]. A similar relation also holds for any linear combination of statistical tensors,

$$\lim\left\{\sum_\lambda A_\lambda[\rho_0^\lambda - \rho_0^\lambda(eq)]\right\}$$

$$= -(1/T_\mu)\left\{\sum_\lambda A_\lambda[\rho_0^\lambda(t) - \rho_0^\lambda(eq)]\right\} \quad (44)$$

This result is independent of whether or not a spin temperature exists [see Eq. (8)].

(ii) T_μ is temperature independent. The relation

$$T_\mu H = \text{const} = Ck/\mu \quad (45)$$

is analogous to the Korringa relation $T_1 T = C$, but expresses the fact that the relaxation rate depends on the magnetic, rather than thermal, energy. Equation (45) should hold true both for ordinary metals and for ferromagnetics, provided that H is the net field at the nucleus.

(iii) T_μ contains the same information that T_1 does. It is clear that both contain the Korringa constant C . It is perhaps less obvious that both yield the nuclear spin. In fact both do, if combined with a suitable set of auxiliary experiments.

(iv) Finally, the approach of T'_1 to constancy occurs at a temperature that is approximately a factor of $2I$ higher than the temperature at which T_1 approaches constancy. This is illustrated in Fig. 1. The practical consequence is that for the range of parameters commonly encountered in nuclear orientation experiments T'_1 easily reaches a saturation value, provided that I is large, while T_1 barely shows any evidence of saturation. Of course T'_1 may not be equal to T_μ even after T'_1 appears to have reached a saturation value.

In view of the above properties of T'_1 and T_μ , we advocate analysis of very low-temperature relaxation data in terms of the relaxation time T_μ rather than the parameter T_1 .

Figure 2 summarizes the rate-equation approach to relaxation theory outlined in this section.

III. EXPERIMENTAL RESULTS

In this section we present the results of relaxation studies based on the observation of radiation patterns from nuclei oriented at low temperatures.

In 1966, Templeton and Shirley³ showed that a substantial decrease in the degree of orientation of nuclei at low temperatures could be obtained by frequency modulating the applied rf power, and that spin-lattice relaxation could be observed by switching off the frequency modulation and watching the angular distribution of emitted radiation decay back to its equilibrium value. The rf power level was maintained constant to ensure a constant lattice temperature T_L during relaxation. The method is summarized in Fig. 3.

The relaxation time is obtained by fitting the decay with an appropriate function, as discussed in Sec. II. At high lattice temperatures the decay is a single exponential with a time constant which is simply related to the rank of the tensor that describes the angular distribution being observed. At low temperatures $T_L \ll h\nu I/2k$ the decay is also to

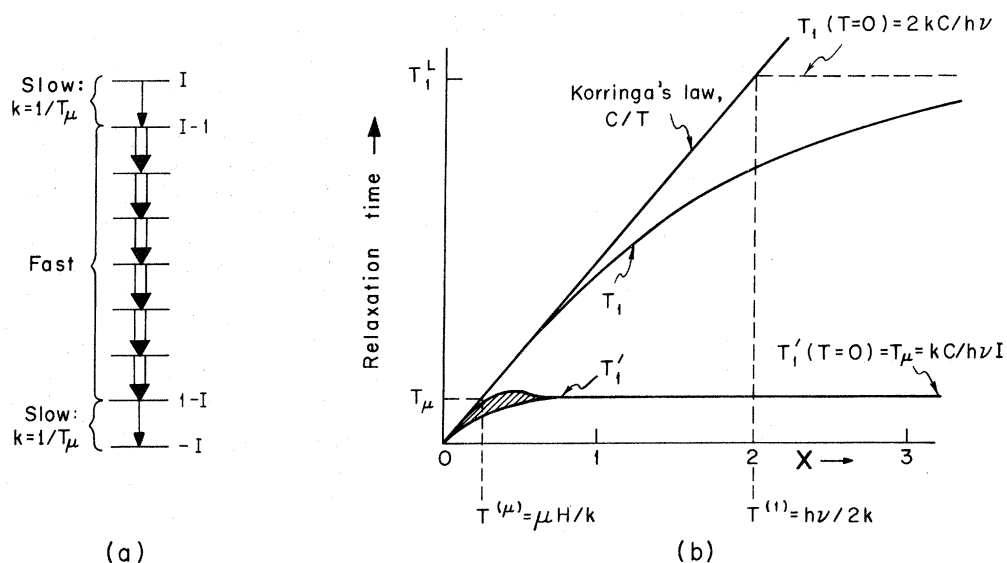


FIG. 1. Comparison of relaxation times T_1 and T_1' . (a) at left represents relative rates of transitions between levels, showing "bottleneck" effect of slower rates between topmost and bottommost pairs of levels, which leads to an effective relaxation time close to T_μ at relatively high temperatures. (b) at right shows temperature behavior of T_1 and T_1' , illustrating the saturation of the latter at a relatively high temperature $T^{(\mu)}$. By similar triangles one sees that $T^{(\mu)}/T^{(1)} = 2I$.

good approximation a single exponential with time constant T_μ . At intermediate temperatures it is a sum of exponentials with various time constants but as explained previously the relaxation rate is controlled by the slowest rate constant after secular equilibrium is reached, and thus the last part of the decay will always be a reasonable approximation to a single exponential. The time required to reach secular equilibrium depends on the initial conditions $\rho_0^A(0)$ and thus if the whole curve from $t=t_0$ onward is fitted with a single exponential, the resulting time constants T_1' will be rather sensitive to initial conditions, except at very high or very low temperatures. [Of course the full multiexponential form, Eq. (31), may be used to fit the decay and obtain T_1 but this procedure is also sensitive to initial conditions as may be seen from Eq. (32).] The initial conditions are, in turn, influenced by the distribution of source nuclei in the sample, the presence of impurities, lattice defects, and surface irregularities, the rf skin depth, and the rf power level and modulation. Moreover, the only knowledge of initial conditions in the sample comes from the anisotropy measurement at $t=t_0$, which is an integral measurement of averages over the whole ensemble of decaying nuclei of the above variables. Thus it is important for reliable relaxation measurements that (a) the initial conditions be kept as constant as possible throughout the experiments and (b) the relaxation curves be fitted with single-exponential functions, the starting point for fitting being $t > t_0$ and approaching $t = t_0$ only at very low

temperatures. The proper starting point for fitting can easily be found by varying the starting points and checking for consistency of the resulting T_1' values. It is our experience that fitting with a multiexponential function to find T_1 is likely to give erratic results due to the lack of accurate knowledge

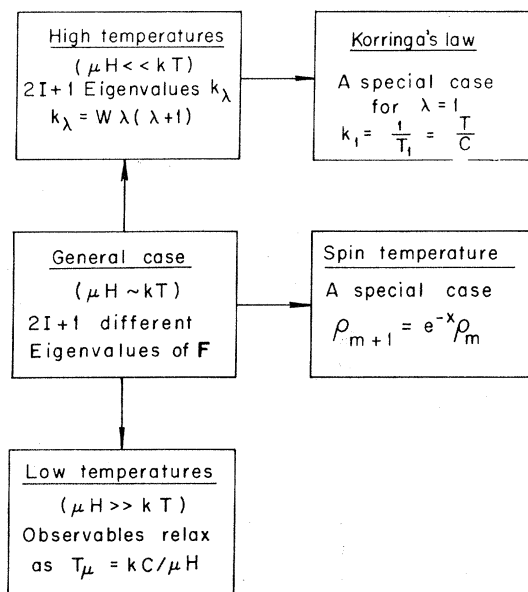


FIG. 2. Block diagram outlining rate-equation relaxation theory and showing relationship of Korringa's law to general theory.

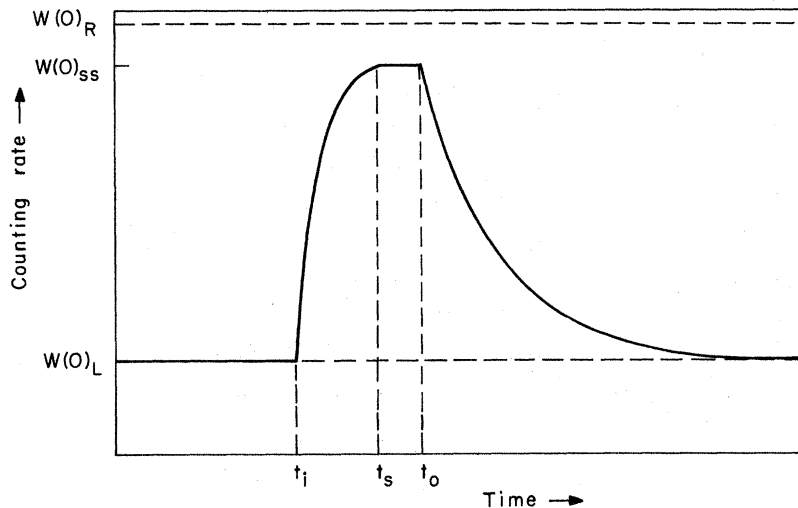


FIG. 3. Illustration of T_1 measurement using NMR/ON with frequency modulation. The counting rate along the polarization axis is denoted as $W(0)$. Subscripts denote the values of $W(0)$ when the nuclei are in thermal equilibrium with the lattice [$W(0)_L$], in a partially disoriented steady state [$W(0)_{SS}$], or randomly oriented [$W(0)_R$]. At time t_i the fm is turned on, causing resonant destruction of the nuclear orientation in the inhomogeneously broadened line. At t_s the resonance is saturated, giving a steady state counting rate $W(0)_{SS}$. At t_o the fm is turned off and the nuclear spins relax back to equilibrium with the lattice. All or part of this relaxation curve can be fitted to obtain either T_1 or T_1' .

of initial conditions. More important, T_1 is not a relaxation time, in an operational sense, at very low temperatures.

Figure 4 shows the experimental results for $^{60}\text{CoFe}$ obtained by the method described above. The T_1' values are those given in Ref. 6; the T_1 values (from multiexponential fits) are previously unpublished. The large scatter in T_1 is a result of variations in initial conditions. The results may be compared with those of Spanjaard *et al.*,¹³ who used the method of rapid eddy-current heating of

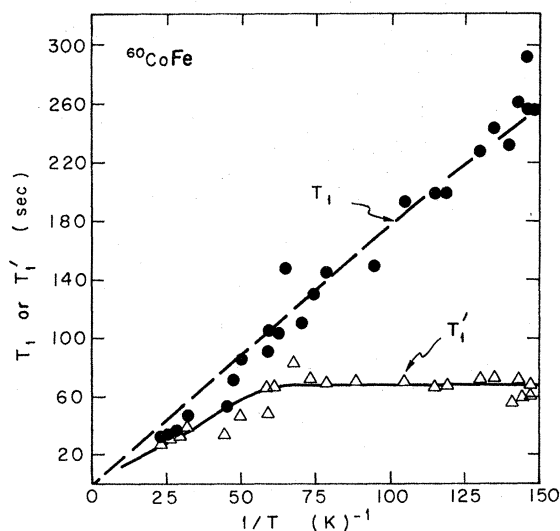


FIG. 4. Relaxation data for $^{60}\text{CoFe}$ at low temperature. The multiexponential-fit T_1 points, indicated by circles, are from Ref. 7; the single-exponential fit T_1' points (triangles) are from Ref. 6. The dashed curve shows the expected hyperbolic tangent dependence of T_1 . The solid curve is simply an empirical curve drawn through the T_1' data.

the sample to obtain relaxation curves.⁴ From the slope of the T_1 -vs- $1/T$ curve one can evaluate the Korringa constant C ; in Table I the value so obtained is compared with a value estimated from T_1' , using $T_1' \approx T_\mu = kC/h\nu I$, and with the value given by Spanjaard *et al.*¹³

Figure 5 shows similar results obtained by Bacon and Brewer²⁴ for $^{56}\text{CoFe}$. The sources were made by the reaction $^{56}\text{Fe}(p, n)^{56}\text{Co}$ on thin polycrystalline Fe foils. After irradiation the foils were annealed and mounted in the NMR/ON apparatus. The resonance, at 209.0 ± 0.2 MHz, had full width at half-maximum (FWHM) of 1.6 MHz

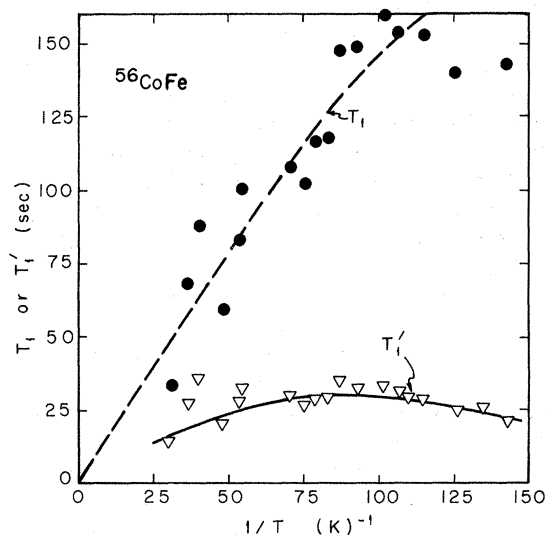


FIG. 5. Relaxation data for $^{56}\text{CoFe}$. The triangles indicate the single-exponential T_1' fit and the circles the multiexponential fit. The dashed curve shows the hyperbolic tangent dependence expected for T_1 .

TABLE I. Derived Korringa constants.

Case	ν_0 (MHz)	T_1' (sec) ^a	C from T_1' (K sec) ^b	C from slope (K sec) ^c	C (other work) (K sec)	Ref.
⁶⁰ CoFe	165.7(2)	67(5) ^d	2.5	1.76(10)	2.6(2)	13
⁵⁶ CoFe	209.0(2)	~25	1.0	1.46(10)	1.1 or 1.6	e
⁶⁰ CoCo	125.1	23(2)	0.69	0.54(7)	0.75	f
⁶⁰ CoNi	69.08(5)	15(3)	0.25	...	0.50(5)	13

^aAverage of low-temperature values in saturation range.

^bUsing $C \cong h\nu T_1'/k$, which approaches being exact as $T_1' \rightarrow T_\mu$.

^cAs $1/T \rightarrow 0$, $T_1 T \rightarrow C$. Errors given are random only.

^dErrors in last digit given parenthetically.

^eCalculated from $C_{56} = (\nu_{60}/\nu_{56})^2 C_{60}$.

^fReference 8, p. 78. The value 0.75 was obtained from NMR data on stable ⁵⁹Co, using $C_{60} = (\nu_{59}/\nu_{60})^2 C_{59}$.

and a maximum of about 55% of the anisotropy could be destroyed by frequency-modulated rf power. We note that somewhat higher rf power levels are required for this experiment than for ⁶⁰CoFe because of the higher resonant frequency and shorter relaxation time of ⁵⁶CoFe. The T_1' values for ⁵⁶CoFe in the temperature range from $1/T = 30$ to 115 K^{-1} do not reach a constant value. Instead they seem to show a maximum as described in Sec. II G. This effect results from the fitting of the *entire* decay curve with a single-exponential function; the percentage of anisotropy destroyed at $t = t_0$ varies by more than a factor of 2 for the data shown in Fig. 5, being about 55% at $1/T = 30 \text{ K}^{-1}$ and only 26% at $1/T = 115 \text{ K}^{-1}$. The initial shape of the decay curves (before secular equilibrium is established) is quite sensitive to this percentage and the T_1' fits are accordingly affected. Consideration of the detailed shape of the curve shows that when the initial resonant destruction of orientation is large, a single-exponential fit to the whole curve will give an erroneously large value of the time constant; this accounts for the "hump" in the T_1' values in Fig. 5. Attempts were made to obtain T_1' at lower temperatures but the low rf power levels consistent with maintaining low sample temperatures were insufficient to produce a reasonable degree of resonant destruction.

As before, the slope of the T_1 values can be used to calculate C , the result being 1.46 sec K. This value may be compared with the value obtained from the ⁶⁰Co measurements by using

$$C_{60}/C_{56} = (\nu_{56}/\nu_{60})^2,$$

i. e., $C_{56} = 1.1$ or 1.6 sec K. Our value of T_1' gives an estimate of $C_{56} \sim 1.0$ sec K.

Figure 6 shows data for ⁶⁰CoCo obtained by Barclay^{8,12} using single-crystal films of cubic Co. These data were analyzed for T_1 using Gabriel's theory, as reported in Ref. 12. An attempt was made to keep the initial conditions constant over the temperature range studied; this was feasible because of the relatively low resonance frequency

of 125.1 MHz and good resonant destruction obtainable. The resulting T_1' curve becomes constant near $1/T = 100 \text{ K}^{-1}$, giving a limiting value for T_1' of 23 ± 2 sec.

Finally, we give the results for relaxation of ⁶⁰Co in single-crystal nickel obtained by Barclay.⁸ First attempts to find the resonance in polycrystalline Ni foil failed, apparently because of excessive inhomogeneous broadening of the resonance line. Later attempts using ⁶⁰Co diffused into a Ni single crystal and for ⁶⁰CoNi uniaxially electroplated onto a single-crystal Cu substrate gave resonance lines at $\nu_0 = 69.08 \pm 0.05$ MHz with FWHM from 0.6 to 1.2 MHz. Some experiments with the plated foils showed anomalies in the magnetization curves (magnetic "hardness" and switching of the easy magnetization direction) which were probably due to differential thermal contraction of the Ni foil and the Cu substrate on cooling. Only about 15% of the anisotropy could be destroyed at toler-

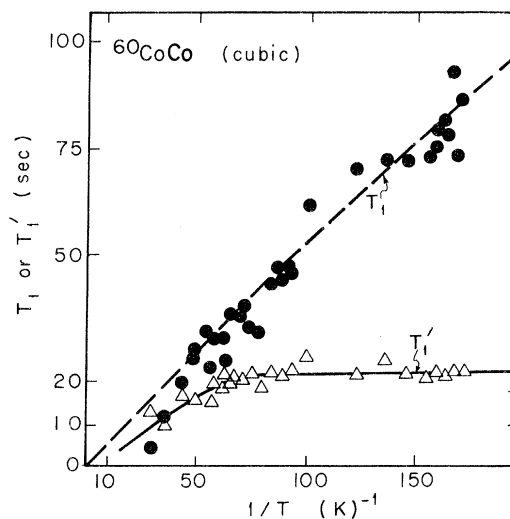


FIG. 6. Relaxation data for ⁶⁰CoCo from Ref. 12. Here the circles, triangles, and curves have the same meanings as in Figs. 4 and 5.

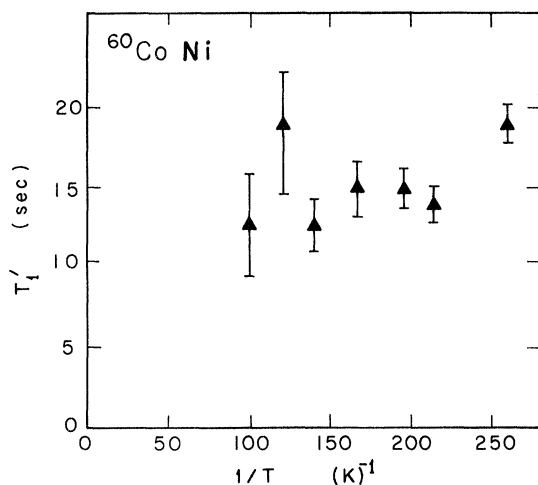


FIG. 7. Relaxation data for $^{60}\text{CoNi}$ (single crystal). Only T_1' is shown: An average value of 15 ± 3 sec was inferred from these data.

able rf power levels. The T_1' values obtained are shown in Fig. 7. These data show large scatter, again due to unavoidable variations in initial conditions and to fitting the whole decay curve with a single-exponential function. Assuming that T_1' is constant, we find $T_1' = 15 \pm 3$ sec.

The values of Korringa constants C and magnetic relaxation times T_1' obtained from these experiments are summarized in Table I and compared with results obtained by other workers. Examination of the last three columns of Table I shows that the values of C obtained in different ways are in quali-

tatively good agreement. A trend is obvious: Relaxation rates for ^{60}Co increase as the host lattice is changed from Fe to Co to Ni. From the resonant frequencies alone one would expect the opposite trend. However, relaxation rates depend on the density of states at the Fermi energy $N(E_F)$ as well as on frequency. Thus we conclude $N(E_F)_{\text{Ni}} > N(E_F)_{\text{Co}} > N(E_F)_{\text{Fe}}$. We also note that the values of C as obtained from the single-exponential fits are in approximate agreement with those obtained by other methods. Detailed quantitative agreement among the various values of C in Table I is not yet available. Further work is necessary to establish where the errors lie in each case.

IV. ON-RESONANT DESTRUCTION OF ORIENTATION AND FREQUENCY MODULATION

In this section we address ourselves briefly to the question: "Why can the nuclear orientation not be completely destroyed?" It has been shown in a number of favorable NMR/ON cases that the orientation could be nearly destroyed (i.e., perhaps 80% destroyed), but there is always some orientation left even in the best cases. This problem has been^{8,25} or will be²⁶ discussed elsewhere in the context of frequency-modulation phenomena. For this reason an extensive treatment would be unwarranted here: We shall simply list and comment on several problems that arise in trying to destroy nuclear orientation resonantly. Most of our remarks apply to the case of a wide inhomogeneously broadened resonance line that must be frequency modulated in order to observe any resonance.³ For

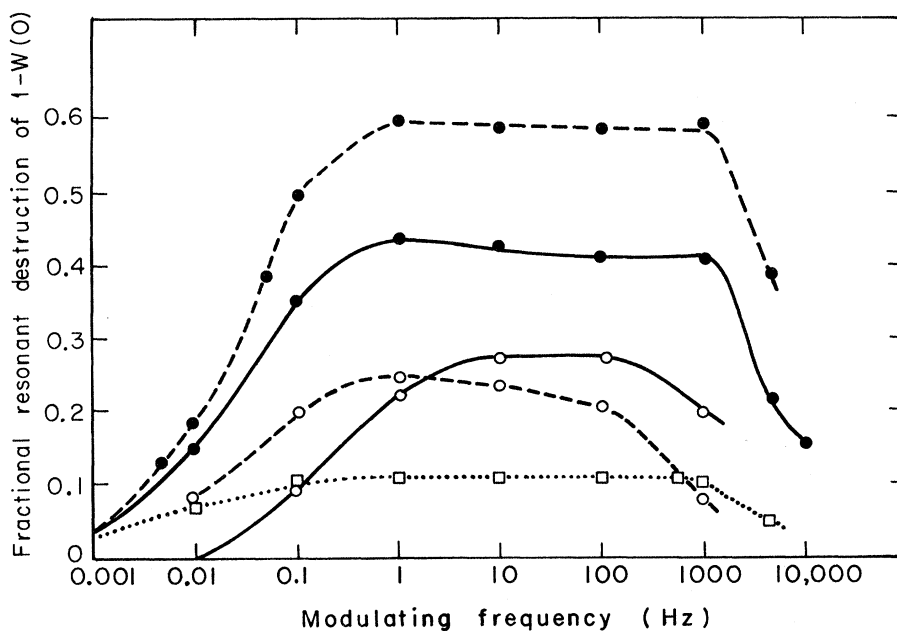


FIG. 8. Fractional destruction of $1 - W(\theta)$, the nuclear orientation "effect," for $\theta = 0$, plotted against the modulation frequency. Filled circles represent $^{60}\text{CoFe}$, open circles $^{60}\text{CoNi}$. Solid curves connect points for which $T_{\text{av}}^{-1} = 95 \text{ K}^{-1}$, and $H_1 = 5.6 \text{ mOe}$; dashed curves connect points for which $T_{\text{av}}^{-1} = 240 \text{ K}^{-1}$ and $H_1 = 1 \text{ mOe}$. In both samples the carrier frequency was centered around resonance [$\nu(^{60}\text{CoFe}) = 166.0 \text{ MHz}$, $\nu(^{60}\text{CoNi}) = 69.1 \text{ MHz}$].

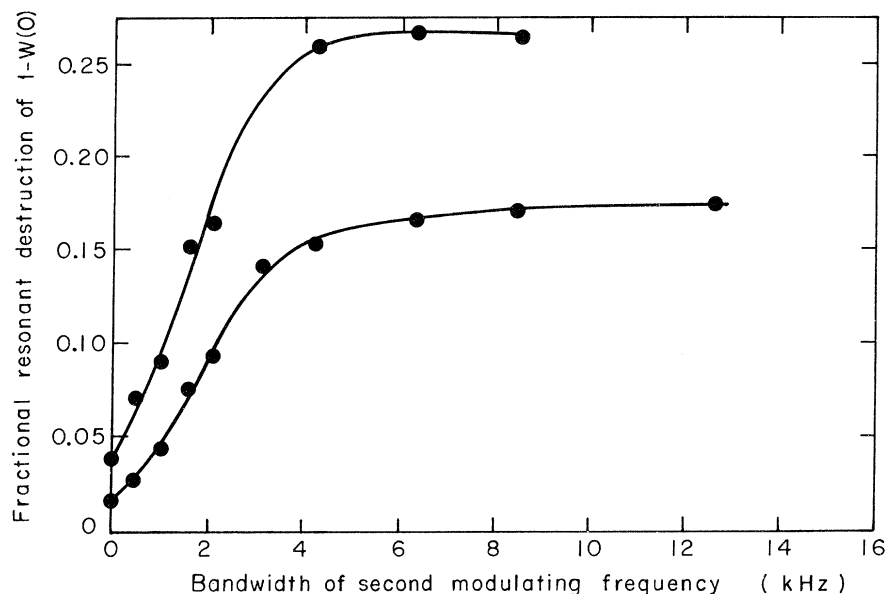


FIG. 9. Fractional destruction of $1 - W(0)$ for $^{60}\text{CoFe}$, with an applied rf field of frequency 165.4 MHz, modulated to a bandwidth of 650 kHz by an applied modulation of frequency $\nu_{fm1} = 5$ kHz. The carrier frequency is also modulated at an audio frequency of 20 Hz through a variable bandwidth $\Delta\nu_2$, shown as abscissa. For the top curve H_1 (applied, peak to peak) = 2.8 mOe and $1/T = 175 \text{ K}^{-1}$. In the bottom curve $H_1 = 1$ mOe, $1/T = 250 \text{ K}^{-1}$.

clarity we shall refer to this as the "resonant region," and to the homogeneous lines of which it is composed as "lines."

First, in successive sweeps through the resonant region, the effects of the rf field on individual lines will add incoherently. For any set of experimental conditions a steady state is quickly established in which orientation is reestablished by relaxation to the lattice at the same rate that it is destroyed by the rf field. Numerical calculations based on an approximate model (but using a realistic set of parameters) show that only $\sim 65\%$ destruction of the orientation parameter B_2 can be expected at 0.002 K even for a favorable case in which the relaxation time is 100 sec and rf-field strength 0.1 G.²⁷

Next, in order to be effective, the modulation frequency ν_{fm} must be neither too low²⁵ nor too high.⁸ If ν_{fm} is too low the nuclei have time to reorient substantially between sweeps. This result was predicted by Wilson, and it has been observed for $^{60}\text{CoFe}$ and $^{60}\text{CoNi}$, as shown in Fig. 8. Also apparent from this figure is a decrease in resonance destruction of anisotropy at high frequencies. This result was postulated as arising from the fact that, as ν_{fm} increases, the frequency-modulation side-

band spacing eventually exceeds the effective linewidth of the homogeneous lines. Some of these lines then fall between sidebands, where they are not excited by the rf field. To test this explanation a separate experiment with $^{60}\text{CoFe}$ was carried out, in which the carrier frequency was modulated by a second, audio frequency $\nu_{fm2} = 20$ Hz, while holding ν_{fm1} constant at 5 kHz. The results are shown in Fig. 9. As expected, resonant destruction of the anisotropy increases with $\Delta\nu_2$, the bandwidth of the second modulation signal $fm2$. The effect is completely restored when $\Delta\nu_2$ exceeds ν_{fm1} . Restoration occurs faster at a higher H_1 amplitude since the intrinsic lines are more power-broadened in this case.

Finally, the intrinsic lines are not simply Lorentzians, but show multipole structure,¹⁹ if even-rank statistical tensors such as B_2 are studied through γ -ray anisotropy measurements. For this reason a hard-core value of alignment exists even at the resonant frequency. One would then expect that any attempt to saturate the resonant destruction effect would result in some of the intrinsic lines exhibiting the "hard-core" response function, thereby yielding an incomplete destruction of the nuclear orientation.

*Work done in part under the auspices of the U. S. Atomic Energy Commission. It was also supported in part by the National Science Foundation while one of us (D.A.S.) was a Senior Postdoctoral Fellow at the Free University, Berlin.

†Present address: Department of Physics, Monash University, Clayton, Victoria, Australia.

‡Present address: I. Physikalisches Institute, Freie Universität, Berlin.

§Present address: Oxford Instrument Corp., 100

Cathedral St., Annapolis, Md. 21401.

¹N. Bloembergen and G. R. Temmer, *Phys. Rev.* **89**, 883 (1953).

²E. Matthias and R. J. Holliday, *Phys. Rev. Letters* **17**, 897 (1966).

³J. E. Templeton and D. A. Shirley, *Phys. Rev. Letters* **18**, 240 (1967).

⁴See, e.g., N. J. Stone, in *Hyperfine Interactions in Excited Nuclei*, edited by G. Goldring and R. Kalish (Gordon and Breach, New York, 1971).

⁵J. A. Cameron, I. A. Campbell, J. P. Compton, and R. A. G. Lines, *Phys. Letters* **10**, 24 (1964).

⁶W. D. Brewer, D. A. Shirley, and J. E. Templeton, *Phys. Letters* **27A**, 81 (1968).

⁷W. D. Brewer, D. A. Shirley, and J. E. Templeton (unpublished). This approach was partially described in Ref. 8, pp. 21-29.

⁸J. A. Barclay, Lawrence Radiation Laboratory Report No. UCRL-18986, 1969 (unpublished).

⁹H. Gabriel, *Phys. Rev.* **181**, 506 (1969).

¹⁰F. Hartmann-Boutron and D. Spanjaard, *Compt. Rend.* **268B**, 1260 (1969).

¹¹D. Spanjaard and F. Hartmann-Boutron, *Solid State Commun.* **8**, 323 (1970).

¹²J. A. Barclay and H. Gabriel, *J. Low Temp. Phys.* **4**, 459 (1971).

¹³D. Spanjaard, R. A. Fox, I. R. Williams, and N. J. Stone, in Ref. 4.

¹⁴T. Moriya, *J. Phys. Soc. Japan* **19**, 681 (1964).

¹⁵R. E. Walstedt, *Phys. Rev. Letters* **19**, 146 (1967); **19**, 816(E) (1967).

¹⁶D. A. Shirley, in *Hyperfine Interactions and Nuclear*

Radiations, edited by E. Matthias and D. A. Shirley (North-Holland, Amsterdam, 1968), pp. 843-858.

¹⁷C. P. Slichter, *Principles of Magnetic Resonance* (Harper and Row, New York, 1963), pp. 118-121.

¹⁸P. Jauho and P. V. Pirila, *Phys. Rev. B* **1**, 21 (1970).

¹⁹E. Matthias, B. Olsen, D. A. Shirley, R. M. Steffen, and J. E. Templeton, *Phys. Rev. A* **4**, 1626 (1971).

²⁰A. Abragam and R. V. Pound, *Phys. Rev.* **92**, 943 (1953).

²¹This is a special case, for $q=q'=0$, of Eq. (16) in Ref. 19. The complex conjugate notation is introduced there for consistency with earlier work.

²²Reference 8, pp. 81-87.

²³In Ref. 6, the symbols W_+ and W_- in the figure, which are referred to here, are different from those in their Eq. (2), which are our $W_{m,m\mp 1}$. The signs in the matrix elements in their Eq. (2) should all be inverted.

²⁴F. Bacon and W. D. Brewer (unpublished).

²⁵G. V. H. Wilson, *Phys. Rev.* **177**, 629 (1969).

²⁶J. A. Barclay *et al.* (unpublished).

²⁷Reference 8, pp. 35-43, and Fig. 10.

Envelope Modulation in Spin-Echo Experiments

W. B. Mims

Bell Telephone Laboratories, Murray Hill, New Jersey 07974

(Received 8 October 1971)

Expressions have been obtained for the envelope-modulation effect in spin-echo experiments of the two- and three-pulse type by partitioning the matrices which describe the evolution of the quantized system. The initial results are quite general and may be applied to a variety of systems. Simplified expressions are derived for the case of an electron spin transition split by small nuclear hyperfine interactions. The results are given in matrix product form. The problem of computing the envelope-modulation parameters in specific instances is discussed. Algebraic results are given for $S=\frac{1}{2}$, $I=\frac{1}{2}$ and $S=\frac{1}{2}$, $I=1$.

I. INTRODUCTION

In spin-echo experiments a periodic variation of amplitude or "modulation" associated with small splittings of the resonance line is sometimes observed in the envelope of echoes.¹ This modulation effect has been used to measure splittings which could not be seen by cw methods because they were too small to be resolved in the presence of inhomogeneous line broadening. Examples in the field of nuclear resonance are the measurement of the $\mathfrak{J} \vec{I}_1 \cdot \vec{I}_2$ coupling^{2,3} in organic molecules and in metals,⁴ and the measurement of nuclear quadrupole coupling.^{5,6} Here we shall be primarily concerned with electron spin echoes, where modulation effects are due to coupling between electron spins and nuclei in the host lattice, i. e., to the superhyperfine structure (shfs) of the resonance. Such modulation effects are a common feature of electron spin-echo experiments.⁷⁻⁹

In Secs. II and III the modulation phenomenon is discussed from a general standpoint without reference to any specific system. This helps to focus attention on the origins of the effect, and makes it possible to derive results for two- and three-pulse echoes (stimulated echoes) without undue mathematical complexity. The method of analysis follows closely that which is used in the treatment of a simple two-level system. The basic formulas can be applied in a wide variety of cases covering both nuclear and optical echo phenomena.¹⁰

The general results are applied to the special case of an electron resonance with shfs splitting in Secs. IV and V. The matrix expressions derived in Sec. IV can be used either to obtain a plot of the echo envelope or to find the amplitudes of the frequency components which appear in it. A procedure for performing the necessary calculations is suggested in Sec. VI. Explicit formulas for coupled systems with $S=\frac{1}{2}$, $I=\frac{1}{2}$ and $S=\frac{1}{2}$, $I=1$